Journal of Physics: Conference Series **525** (2014) 012005 doi:10.1088/1742-6596/525/1/012005

Investigation of Vapour Chamber Performance with a Concentrated Heat Source

[2]E. Ravache, [1]S. Siedel, [1,3]R. Kempers, [1]A.J. Robinson
[1]Department of Mechanical and Manufacturing Engineering, Parsons Building, Trinity College Dublin
[2] Université de Lyon, CNRS
INSA-Lyon, CETHIL, UMR5008, F-69621, Villeurbanne, France
Université Lyon 1, F-69622, France
[3]Alcatel-Lucent Ireland, Blanchardstown Business & Technology Park, Dublin 15, Ireland

Email: arobins@tcd.ie

Abstract. This work aims to characterize the performance of a commercially available solid heat sink (SHS) and a vapour chamber heat sink (VCHS) with a small localized heat source. The heat sinks were tested under forced convection conditions in a dedicated wind tunnel. Heat transfer and temperature measurements facilitated the estimation of the source-to-sink thermal resistance whilst thermal imaging on the air side of the heat sink was used to gauge the level of heat spreading. The results indicate that the VCHS was capable of spreading the heat from the localized source over a greater surface area of the heat sink compared with the SHS. However, the improved spreading resistance of the VCHS was offset by the additional contact resistance and/or the thermal resistance of the internal wick structure resulting in a source-to-sink thermal resistance and heater temperature which was commensurate with the SHS. As a result there was no thermal benefit of the VCHS.

1. Introduction

Heat sinks are used as surface area extensions from small electronic components in order to lower the air-side thermal resistance, thus the net source-to-sink thermal resistance. However, there are limits with regard to the size of the heat sink since its effectiveness decreases as it gets larger due to spreading resistance i.e. the temperature of the outer fins decrease as heat is not effectively conducted to them from the source.

One solution to this is the use of a vapor chamber heat sink (Fig. 1) to aid in the lateral spreading of the heat from the localized source to the outer periphery of the heat sink.

As it is illustrated, a VCHS operates as a heat pipe where a working fluid is vaporized within a wick structure at the location of the heat source and condensed in a wick structure in thermal contact with the fin base area. The heat is spread by virtue of the vapor filling the void between the base of the heat sink and the base of the fins. The condensed liquid is returned to the evaporator by means of the wick structure in a manner which is the same as a conventional heat pipe.

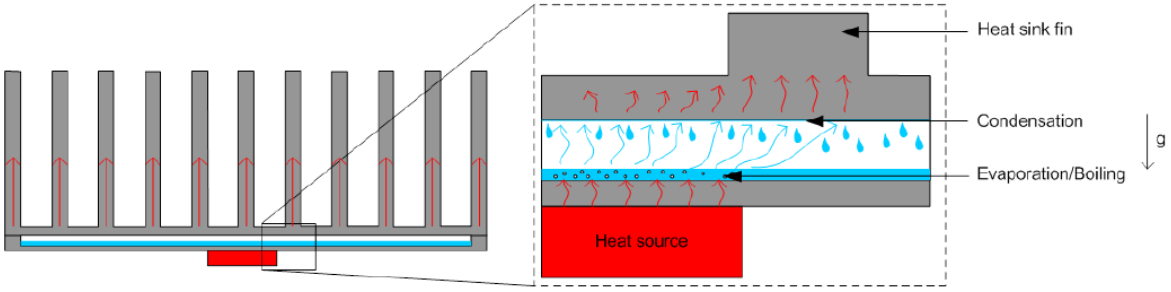

Figure 1. Schematic of a VCHS.

Li et al. [1] compared an aluminum heat sink and a vapor chamber heat sink using infrared thermography. Their results showed that the latter one was more effective with a lower maximum temperature for the same power applied and a lower overall thermal resistance.

Chen et al. [2] compared an aluminum heat sink, a copper heat sink and a vapor chamber heat sink. Once again, the vapor chamber heat sink outperformed the other heat sinks due to its spreading performance. Indeed, they expressed the temperature distribution in terms of the standard deviation and showed that the values associated with a VCHS were lower than for the standard heat sinks. This standard deviation was constant for VCHSs and increased with increasing power for the standard heat sink. Moreover, they showed that the thermal resistance of the VCHS decreases when the power input increases. Conversely, the thermal resistances of the standard heat sinks were constant with respect to the power input.

Boukhanouf et al [3] found similar results and used thermal imaging to show that the thermal spreading resistance of their VCHS was about 40 times lower than that of a similar copper heat sink. Likewise, they showed that the operating temperature was up to 15^{o}C lower than the operating temperature of the copper heat sink for the same heat flux.

Several papers showed that the overall thermal resistance of a VCHS decreases when the power input increases [2, 3, 4, 5]. Conversely, Koito et al. [6] found that the VCHS thermal resistance was constant with respect to the power input and that it decreased as the heat source size became closer to the size of the heat sink. In other studies [5, 6] no comparison was made with solid heat sinks so it is difficult to gauge the benefit of the VCHS.

The results above indicate that VCHSs exhibit lower thermal resistances resulting in lower maximum surface temperatures and that their spreading resistance is smaller than that of a standard heat sink. Even still, as shown by Sauciua et al. [7], it is not always more effective than simply increasing the thickness of the heat sink base plate. In this regard it may be the weight advantage that makes the VCHS more appropriate though this would depend on the particular situation as well as cost considerations.

The design of a VCHS requires careful attention to the design of the wick structure since any gains associated with the heat spreading can be more than offset by the relatively poor effective thermal conductivity of the liquid saturated wick at the evaporator and condenser. This is particularly crucial for concentrated heat sources where the poor effective thermal conductivity is accentuated by a small relative area, which also negatively influences the overall thermal resistance. Further to this, some companies are commercializing VCHSs as ‘bolt-on’ devices. Here special attention must also be paid to the additional thermal contact resistance associated with the vapor chamber and solid heat sink.

In this investigation, commercially available vapor chambers attached to an aluminum extruded heat sink as well as a solid heat sink are investigated under forced convection conditions. Importantly a discrete heat source is tested with variable heat loading so as to gauge the thermal performance of the VCHS against the solid heat sink.

2. Experimental Apparatus

Three heat sinks were tested under identical thermal loading and flow conditions. The SHS was a solid aluminum extrusion of base dimension of 244 x 300 mm^2 with a total of twenty one 4 mm thick and 45mm high fins. The two VCHS's tested were comprised of the same aluminum extrusion with a commercially sourced 'bolt-on' flat vapor chamber fastened to the base. The geometric parameters associated with the VCHS and SHS are outlined in Table 1.

Table 1. Heat sink dimensions.

	Solid heat sink	VCHS
Length (mm)	300	
Width (mm)	244	
Total height (mm)	48	50
Number of fins	21	
Fin Height (mm)	45	
Fin thickness (mm)	4	
Gap between fins (mm)	9	

The geometry of these heat sinks is more optimal for natural convection operation as they are based on the natural convection heat sinks used in Remote Radio Heads (RRH) used in the telecommunications industry. However, for the purposes of these tests, they were tested under forced convection conditions in order to minimize the convective thermal resistance and increase the relative contribution of the heat sink itself to the measured thermal resistance.

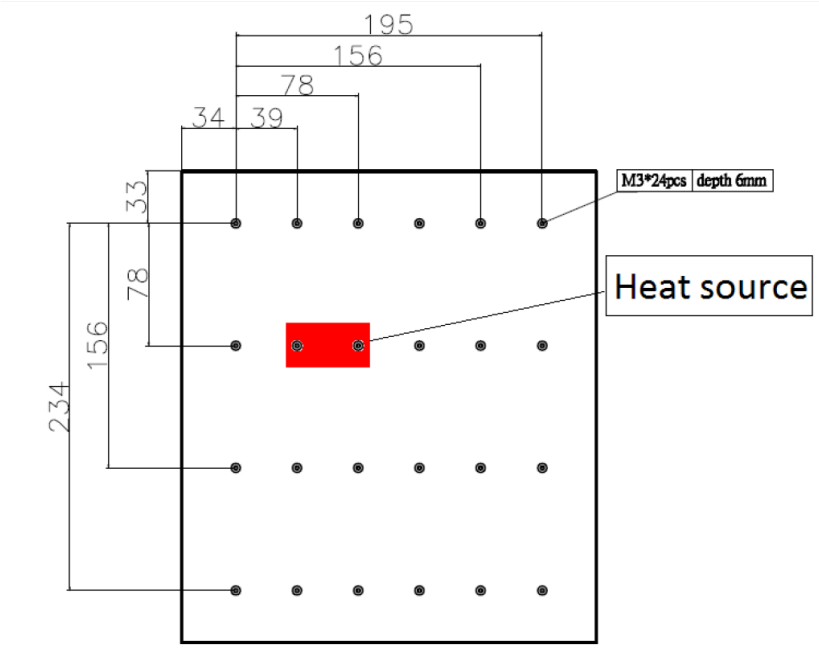

Figure 2. Heat sink base showing heater location and dimensions.

Fig. 2 depicts the base of the heat sink showing the bolt hole locations for affixing the vapor chamber as well as the relative size and location of the heater. Fig. 3 shows the assembled VCHS

along with a cut section of the vapor chamber showing the sintered wick structure on both the evaporator and condenser regions.

Figure 3. Image of the VCHS cross section and overall composition.

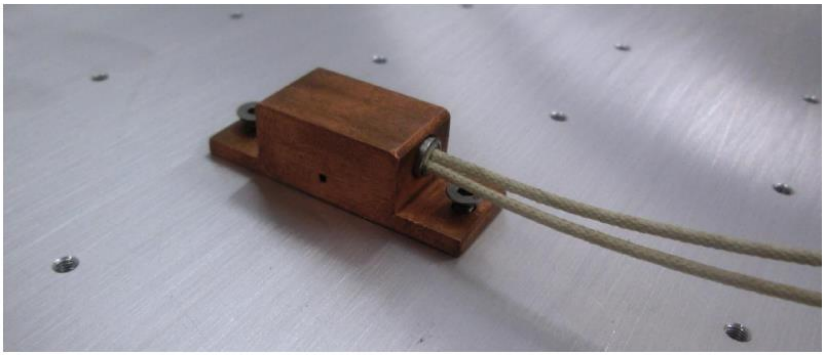

Figure 4. Heat source attached to the heat sink base.

The heat source was designed to have a similar size and power to the heat sources that are cooled by the heat sink in real operation, such as the RF power amplifiers used in Remote Radio Head applications. To this end, heat is applied to a Ø6.35 mm x 25.4 mm cartridge heater. It is inserted into a copper sheath bolted to the heat source side (Fig. 4). Identical assembly torque settings were used for these tests. Power is supplied to the heaters using a variable voltage transformer that can deliver up to 240 V. Although the heat sink has the capacity to accommodate several heat sources, only one was tested in this investigation. Unwanted heat losses were minimized with a thick layer of insulation on the underside of the assembly.

A schematic of the experimental rig is illustrated in Fig. 5. The rig is composed of a centrifugal fan and a purpose built wind tunnel which contains the heat sink under test. Several measurement devices

were used such as an infrared camera, thermocouples, Pitot probe and voltage and current meters. A dedicated computer with DAQ hardware (National Instruments) and software (LabView, ThermaCAM Researcher Professional 2.9) recorded relevant data required for the calculation of the overall source-to-sink thermal resistance.

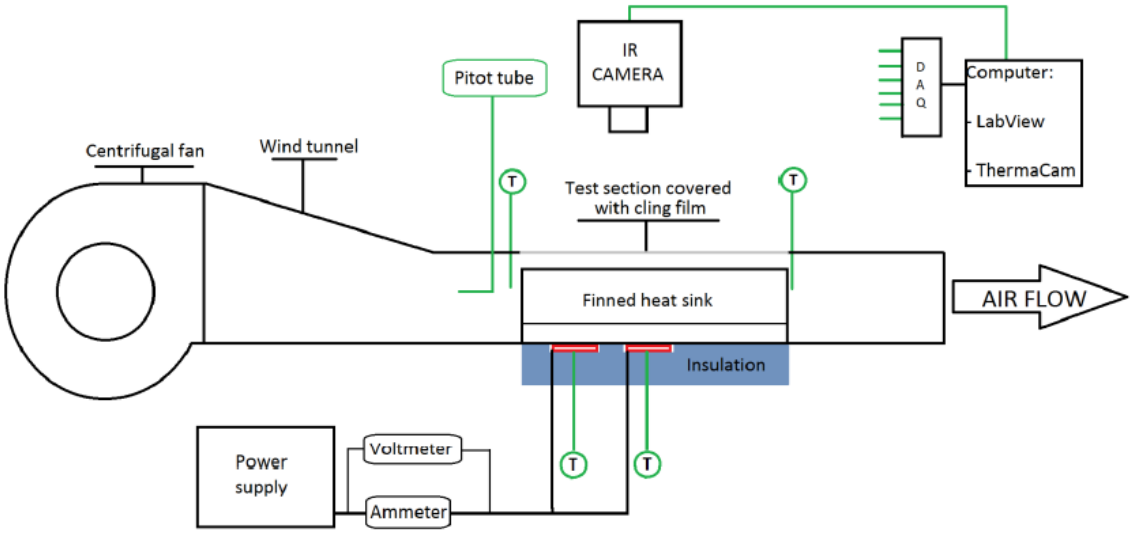

Figure 5. Schematic of the experimental apparatus.

3. Data Reduction

The supplied power Q_{in} was determined from current and voltage measurements taken with digital multimeters. Since heat losses were minimal, a sufficiently accurate estimation of the heat input can be calculated simply as,

$$Q_{in} = IV \tag{1}$$

Using expressions of thermal resistances proposed by Yovanovich and Marotta [8] and Webb [9], the overall thermal resistance of a heat sink can be expressed as a function of the power input and the log-mean temperature difference,

$$R = \frac{\Delta T_{lm}}{Q_{in}} \tag{2}$$

where the log-mean temperature difference is given by,

$$\Delta T_{lm} = \frac{(T_s - T_{air,in}) - (T_s - T_{air,out})}{\ln\left[\dfrac{(T_s - T_{air,in})}{(T_s - T_{air,out})}\right]} \tag{3}$$

Here, T_s is the source temperature and $T_{air,in}$ and $T_{air,out}$ are the inlet and outlet air temperatures respectively. The temperatures are time averages of 500 measurements once steady state conditions were achieved.

4. Results and Discussion

The performance of the heat sinks was characterized by comparing the various performance metrics such as the overall source-to-sink thermal resistance, heat spreading and source temperature.

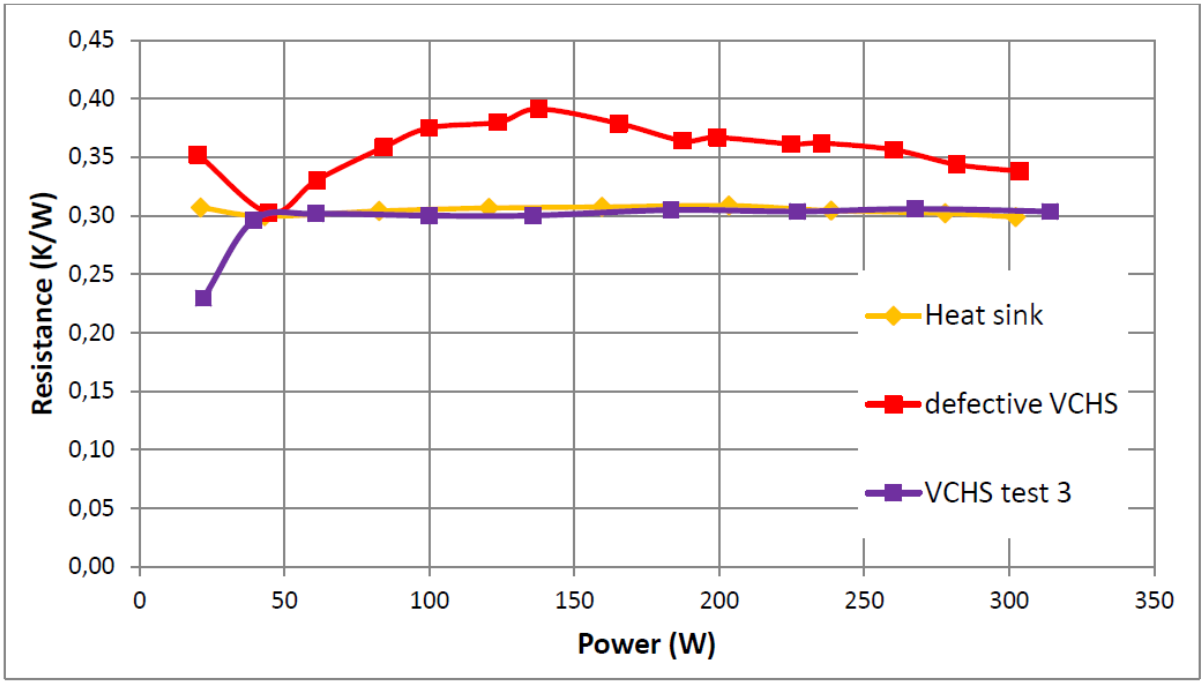

Figure 6. Plot of thermal resistance versus heat load.

Fig. 6 shows the overall source-to-sink thermal resistance for the SHS and two VCHS's. It is first noticed that the thermal resistance of the SHS is independent of the imposed power. This is not entirely surprising since the airflow was kept constant for each experiment and the aluminum thermal conductivity varies very little over the temperature range of the experiments. It does, however, indicate that the spreading resistance within the SHS is not a non-linear function of the imposed power or driving temperature differential.

Fig. 6 also shows the thermal resistance for each of the two VCHSs. It is first noticed that there is a notable discrepancy between the two units, and in fact indicates that one of the VCHSs was faulty as it had a notably higher thermal resistance than both the operational VCHS and the SHS. The operational VCHS shows a thermal resistance which, apart from the lowest power load, was not distinguishably different than the SHS.

Fig. 7 shows thermal images taken of the top-side of the heat sinks for heat loads of 40W, 140W and 240W. The left images are of the SHS and the ones on the right are of the operational VCHS. Here, the temperature scale for the false color representation of temperature is allowed to float so as to accentuate the visualization of the heat spreading. The thermal images clearly show that the VCHS has the ability to spread the heat over a significant surface area compared with the more localized footprint of the SHS. However, considering Fig. 8 where the false color temperature scale is the same for each the SHS and VCHS, it is evident that the VCHS is much cooler indicating that the contact resistance between the vapor chamber and the heat sink and/or the resistance in the wick structures are considerable.

The additional thermal resistances associated with the interface between the vapour chamber and the heat sink and/or the low effective conductivity of the wick structures has a net effect that that the improved heat spreading on the air-side is entirely offset by these additional resistances (Fig. 6).

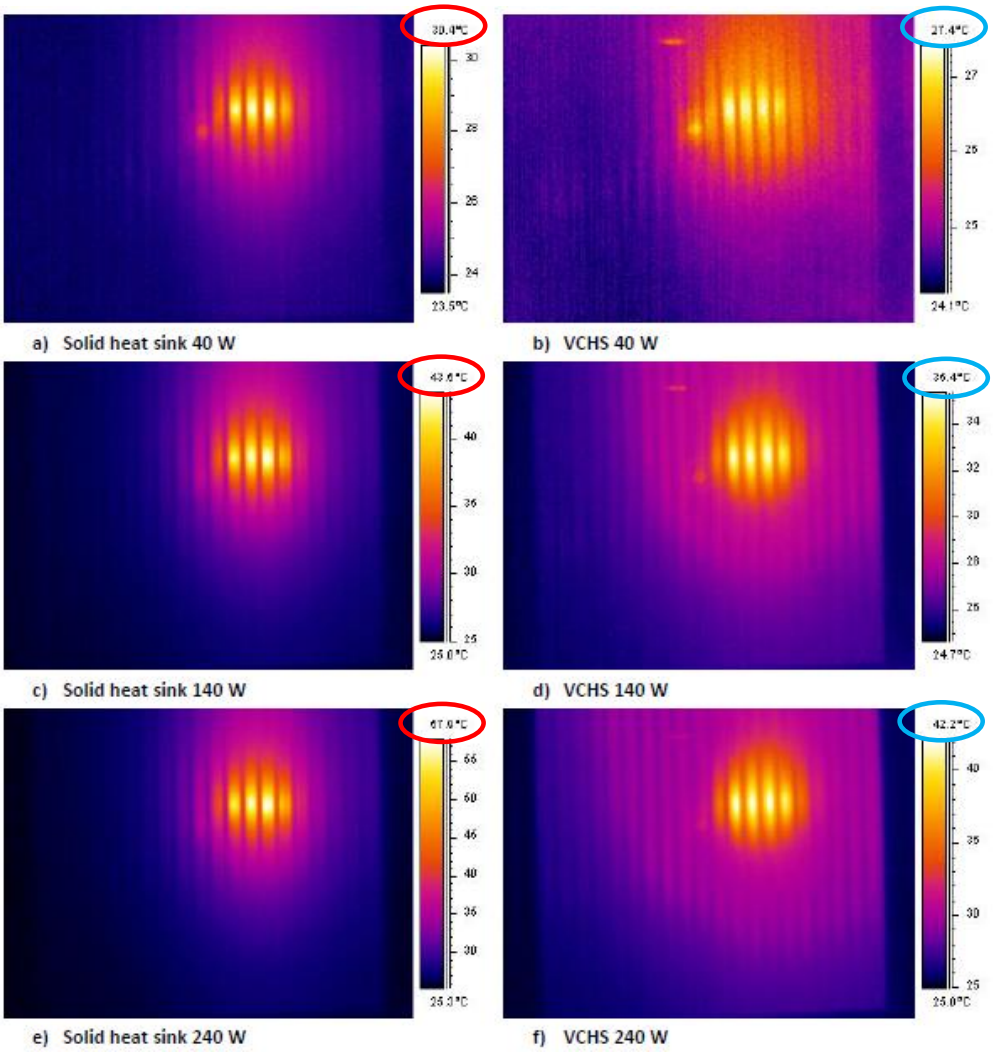

Figure 7. Thermal images showing degree of heat spreading. Floating temperature scales.

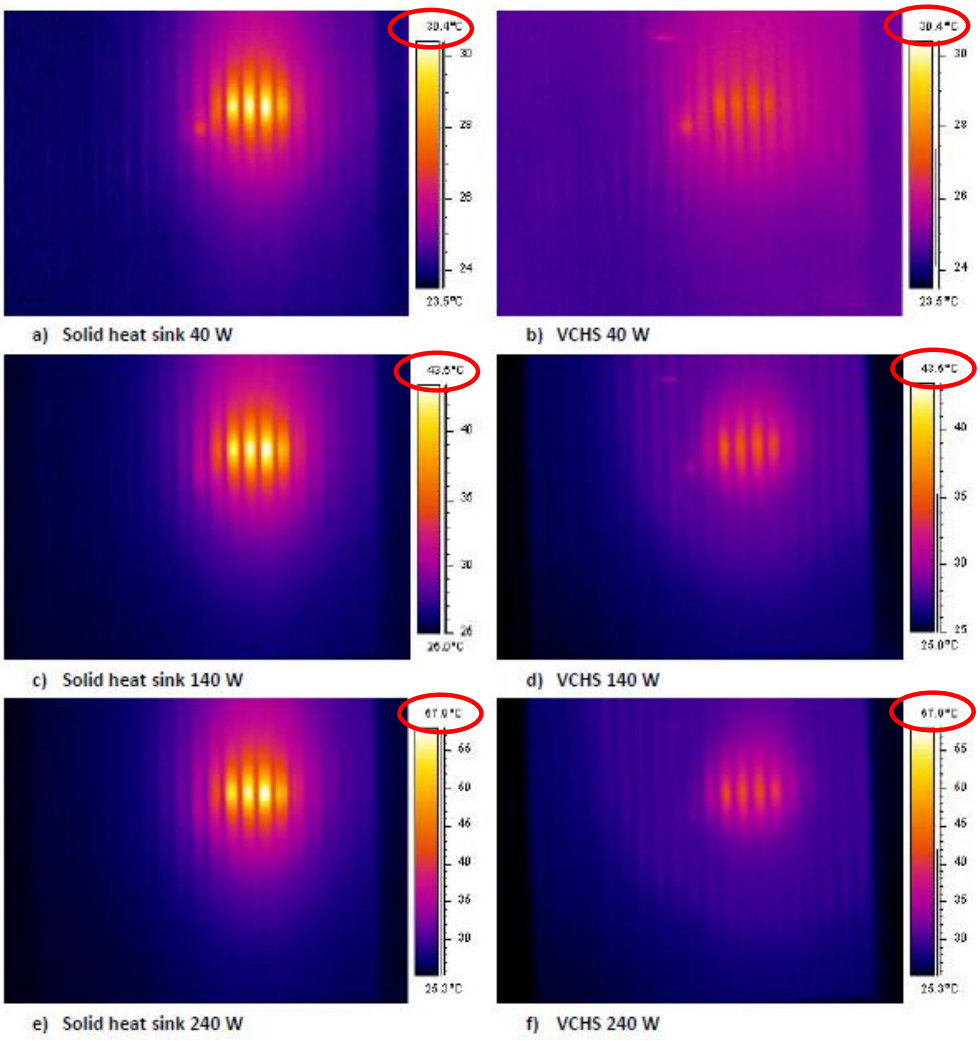

Figure 8. Thermal images showing degree of heat spreading. Fixed temperature scales.

The main purpose of the thermal management system is to keep the source temperature low enough to avoid thermal failure of the electronic component. Even still, other issues such as cost, reliability, complexity and weight are also important in the design of appropriate thermal management systems. Referring to Fig. 9 it is clear that considering all of the aspects mentioned above, this VCHS is a low performing technology. As the figure shows, it does not improve the temperature of the heat source over that of a SHS and in fact worsens the case for one of the two VCHSs tested.

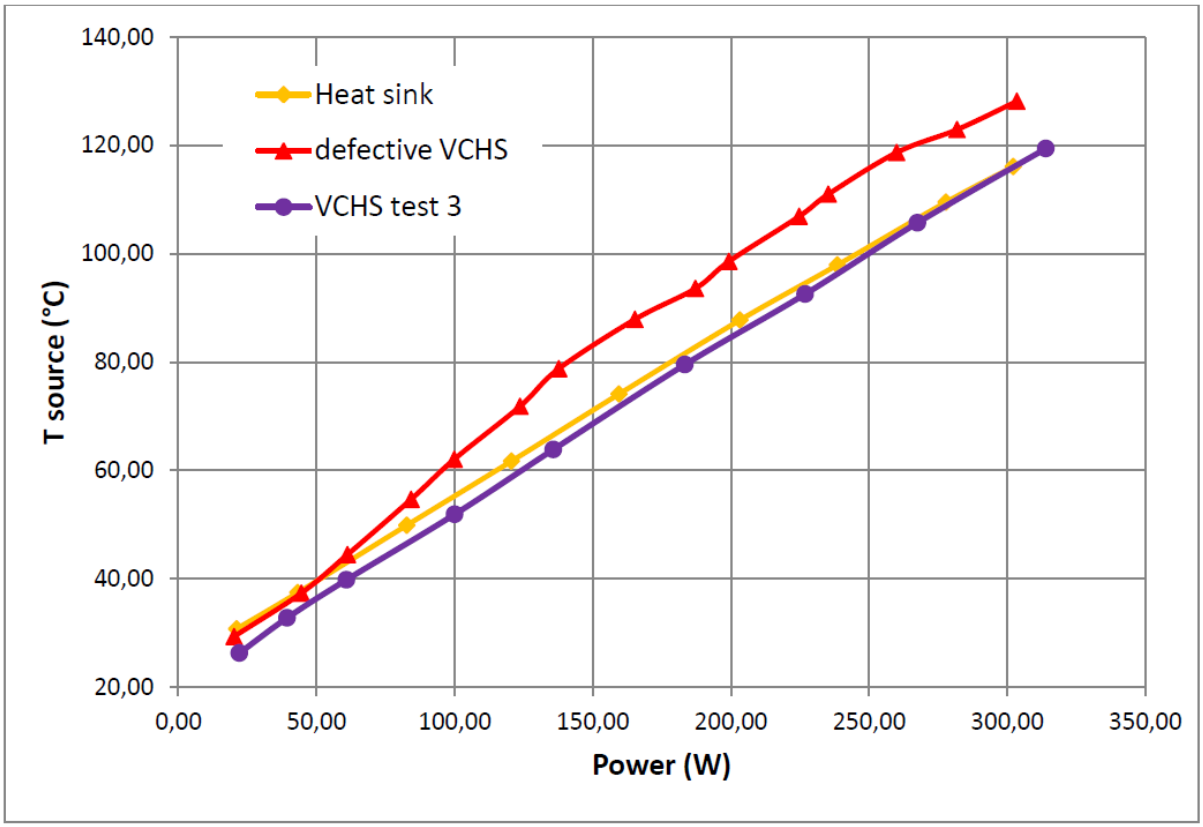

Figure 9. Plot of source temperature versus heat load.

5. Conclusions

The results of this investigation show that 'bolt-on' VCHS's must be used with caution if used with localized heat sources. Although they are effective heat spreaders, they do not necessarily improve the source-to-sink thermal resistance for this scenario. The additional thermal resistances associated with the interface between the vapor chamber and the heat sink together with the wick structures can more than offset any gains associated with the heat spreading. Full integration of the vapor chamber into the heat sink, opposed to the 'bolt-on' system, would of course mitigate the additional contact resistance.

Further, for highly populated boards with a common heat sink the heat spreading may in fact be disadvantageous since the spreading can be considered thermal pollution from high powered components to low powered components on the same heat sink which can compromise device reliability. Another factor to consider is that there are performance limitations, such as the capillary limit, associated with heat pipe types of heat exchangers. In particular, orientation could become a factor and this is not the case with solid heat sinks.

Although VCHSs show promise in terms of becoming another technology in the growing arsenal of advanced thermal hardware for electronics thermal management, more research is still required.

References

[1] Li HY, Chiang M H, Lee C I, Yang W J 2010 Thermal performance of plate-fin vapor chamber heat sinks *Int.Comm.Heat Mass Transfer* 37(7) 731–738

[2] Chen Y S, Chien K H, Wang C C, Hung T C, Ferng Y M, Pei B S 2007 Investigations of the thermal spreading effects of rectangular conduction plates and vapor chamber *J. Electron. Pack*. 129 348–355

[3] Boukhanouf R, Haddad A, North M T, Buffone C 2006 Experimental investigation of a flat plate heat pipe performance using IR thermal imaging camera *Appl. Therm. Eng.* 26 2148–

2156
[4] Tsai M C, Kang S W, Vieira de Paiva K 2013 Experimental studies of thermal resistance in a vapor chamber heat spreader *Appl. Therm. Eng.* 56(1–2) 38–44
[5] Hsieh S S, Lee R Y, Shyu J C, Chen S W 2008 Thermal performance of flat vapor chamber heat spreader *Energy Conversion and Management* 49(6) 1774–1784
[6] Koito Y, Imura H, Mochizuki M, Saito Y, Torii S 2006 Fundamental experiments and numerical analyses on heat transfer characteristics of a vapor chamber (effect of heat source size) *JSME Int. J. Series B* 49 1233–1240
[7] Sauciua I, Chrysler G, Mahajon R 2002 Spreading in the heat sink base: phase change systems or solid metals? *IEEE Trans Compon Pack Technol* 25 621–628
[8] Yovanovich M M, Marotta E E 2003 Thermal spreading and contact resistances, in: A. Bejan, A.D. Kraus (Eds.) Heat Transfer Handbook John Wiley & Sons 261–393
[9] Webb R L Heat Exchanger Design Methodology for Electronic Heat Sinks *J. Heat Transfer* 129(7) 899-901